# Contributions of alanine and serine to sulfuric acid-based homogeneous nucleation

Hui Cao [a], Yi-Rong Liu [a], Teng Huang [b], Shuai Jiang [a], Zi-Hang Wang [a], Ying Liu [a], Ya-Juan Feng [a,**], Wei Huang [a,b,c,*]

[a] School of Information Science and Technology, University of Science and Technology of China, Hefei, Anhui, 230026, China
[b] Laboratory of Atmospheric Physico-Chemistry, Anhui Institute of Optics & Fine Mechanics, Chinese Academy of Sciences, Hefei, Anhui, 230031, China
[c] CAS Center for Excellent in Urban Atmospheric Environment, Xiamen, Fujian, 361021, China

## HIGHLIGHTS

- Synergistic effect enhances pre-nucleation clusters formation.
- Steric effect suppresses pre-nucleation clusters formation.
- Formation rates are positively correlated with the monomers' concentration.
- Formation rates are negatively correlated with temperature.

## ARTICLE INFO

## ABSTRACT

New particle formation (NPF) is the main source of atmospheric aerosols, and amino acids have been detected as the important components of atmospheric particulate matter. However, the role played by amino acids with different functional groups in the initial events of nucleation remains unclear. In this study, the interactions of alanine (Ala) and serine (Ser), which differ structurally by one hydroxyl group, with sulfuric acid were studied at the M06-2X/6-311 + G (d, p) theory level. Structural and thermochemical analysis results show that in small clusters, the introduction of the Ser's hydroxyl groups leads to the synergistic effect, which promotes proton transfer and improves the stability of the clusters. With the increase of cluster's size, the synergistic effect gradually reduces, the introduction of hydroxyl groups hinders the formation of hydrogen bonds between amino and carboxyl groups of Ser molecules with sulfuric acid molecules, resulting in the steric effect, reducing the stability of the clusters. Atmospheric relevance analysis results show that the formation rates of the clusters are positively correlated with the concentrations of sulfuric acid and amino acid, but negatively correlated with temperature. The temperature dependence of $(SA)_m (Ser)_m$ is lower than that of $(SA)_n (Ala)_n$ (n, m = 1–2, n = m), indicating for small clusters, the synergistic effect improves the stability of the clusters and plays an important role in the formation rates. The formation rates of $(SA)_m (Ser)_m$ are slightly lower than that of $(SA)_n (Ala)_n$ (n, m = 3–4), indicating for large clusters, the steric effect reduces the stability of the clusters and the concentrations of amino acid and sulfuric acid, temperature have greater influence on the formation rates.

## 1. Introduction

Nowadays, atmospheric aerosols have received widespread attention for their important effects on human health, visibility, global radiation balance and tropospheric chemistry (Zhang et al., 2007; Kulmala et al., 2004; Saxon and Diaz-Sanchez, 2005; Saikia et al., 2016; Kulmala, 2003; Kalberer et al., 2004). New particle formation (NPF) is an important part of the formation of atmospheric aerosols (Bianchi et al., 2016; Cai and Jiang, 2017; Lin et al., 2019), which contains two main stages: the formation of a critical nuclei and growth of a critical nuclei to larger sizes (>3 nm) (Zhang et al., 2012; Chu et al., 2019; Lee et al., 2019). Although there are actual field measurements, laboratory experiments

---

and theoretical studies of atmospheric aerosols and nucleation events (Zhang et al., 2007; Chu et al., 2019; Lee et al., 2019; Zhang and Anastasio, 2003; Seinfeld and Pandis, 2006; Vaattovaara et al., 2006; Kourtchev et al., 2009; Kalivitis et al., 2019), the size and chemical composition of the critical nuclei remain unclear at the molecular level (Zhao et al., 2010; Jokinen et al., 2012; Junninen et al., 2010; Chen et al., 2017; Li et al., 2019).

While sulfuric acid (SA) is the most common nucleating precursor (Laskin et al., 2003; Sipilä et al., 2010a; Temelso et al., 2012; Al Natsheh et al., 2004; Vehkamäki et al., 2002), whose concentration in the atmosphere explains the rate of atmospheric nucleation at most situations (Sipilä et al., 2010a), there are many other atmospheric nucleation precursors, such as ammonia (Ge et al., 2011; Kurtén, 2006, 2007; Nadykto and Yu, 2007; Ianni and Bandy, 1999), atmospheric ions (Lovejoy et al., 2004; Bork et al., 2012; Herb et al., 2013; Nadykto et al., 2008; Ortega et al., 2008) and organic compounds (Kalberer et al., 2004; Lin et al., 2019; Nadykto and Yu, 2007; Zhang et al., 2004; Wang et al., 2016; Elm, 2013; Elm et al., 2013; Xu et al., 2010; Kurtén et al., 2008; Loukonen et al., 2010; Knopf et al., 2018; Smith et al., 2008), participating in the formation of the critical nuclei, contributing to NPF, and promoting the formation of atmospheric aerosols.

Organic nitrogen compounds are abundant in the atmosphere and have significant effects on terrestrial and aquatic ecosystems, air quality, and climate (Wu and Tanoue, 2002; Cornell et al., 2003; Andreae and Crutzen, 1997; Milne and Zika, 1993; Aber et al., 1989; Fenn et al., 1998). Previous studies have shown that water-soluble organic nitrogen compounds account for about 18% of the total fine particle mass (Zhang et al., 2002). Amino acids are important forms of organic nitrogen compounds and have been detected in urban and marine aerosols, rain, and fog droplets (Zhang and Anastasio, 2001, 2003; Knopf et al., 2018; Kim et al., 2019; Ren et al., 2018; Feltracco et al., 2019; Scheller, 2001; Bianco et al., 2016; Matos et al., 2016). Concretely, glycine is the main amino acid in the quantitative analysis of continental aerosols and marine aerosols in China, with average contents of 83% and 66% of the total amino acids, respectively (Huang et al., 2018). In Northern California, Ornithine is the main component of free amino compounds (FAC) in $PM_{2.5}$ and fog water, typically accounting for 20% of FAC (Zhang and Anastasio, 2003). In Arctic, the total concentration of free amino acids (FAAs) in $PM_{10}$ ranges from 2.0 to 10.8 pmol $m^{-3}$, while combined amino acids (CAAs) ranges from 5.5 to 18.0 pmol $m^{-3}$ (Feltracco et al., 2019). Field measurements have shown that aerosols and particles in the atmosphere are rich in compounds such as arginine, Ala and Ser (Zhang and Anastasio, 2003; Mandalakis et al., 2011). Recently, Elm et al. proposed glycine can act as stabilizers for small clusters containing sulfuric acid, and enhance the formation of the small clusters in two directions in geometrical space (Elm et al., 2013). Then, Wang et al. proposed the amino group in Ala always directly binds with sulfuric acid, while the carboxyl group always binds with water in the hydrated (Ala) (SA) core system (Wang et al., 2016). Moreover, Ge et al. concluded that Ser can form a cyclic structure with sulfuric acid through hydroxyl and amino groups, and play more important role in stabilizing sulfuric acid (Ge et al., 2018). In addition, it has been confirmed by Roosta et al. that the hydrophobic and hydrophilic properties of amino acids have dual effects on the nucleation and growth rate of hydrates (Roosta et al., 2018). Those studies have shown that amino acids can contribute to nucleation (Ge et al., 2018), yet it's not clear whether different amino acids have different influence in enhancing the initial nucleation.

Zhang has proposed that the carboxyl group of organic acids has more oxygen atoms than hydroxyl group, while oxygen atoms can act as the acceptors of non-covalent hydrogen bonds (Zhang et al., 2018). Meanwhile, basic gas can form clusters with sulfuric acids through acid-base neutralization reactions (Li et al., 2019; Ge et al., 2011; Jen et al., 2014). Considering that the basic amino groups and acidic carboxylic groups can coexist in the amino acid molecule during the formation of clusters of amino acids and sulfuric acids, the two functional

groups may have different roles in different nucleation stages, and the functional groups may also affect each other.

In this paper, we choose two amino acids that differ structurally by one hydroxyl group, Ala and Ser, as the objectives and study how they interact with sulfuric acids. We will discuss their roles in the processes of initial nucleation through structural analysis, thermodynamic analysis and atmospheric relevance. Further, we hope to discover the different performances of the two amino acids and explore the roles of different functional groups in the processes. Previous studies have shown that the small (Ala) (SA) cluster is more favorable in low humidity environments (Wang et al., 2016), and Ser as hydrophobic amino acids can reduce the rate of hydrate formation (Roosta et al., 2018). Therefore, we did not include water molecules in the research system.

## 2. Methods

### 2.1. Structural calculations

The initial geometric structures of the $(SA)_n$ $(Ala)_m$ and $(SA)_n$ $(Ser)_m$ (n, m = 1–4) clusters were obtained using the Basin-Hopping (BH) algorithm coupled with semi-empirical PM7 implemented in MOPAC 2016 (Maia et al., 2012; Huang et al., 2010; Wales and Doye, 1997; Hostaš et al., 2013). For each cluster, we sampled 500 local minimum structures, and selected 30 low-energy structures for optimization (Li et al., 2019; Wen et al., 2018; Liu et al., 2014). Then, the stable isomers within 6 kcal $mol^{-1}$ were optimized at the M06-2X/6-311 + G (d, p) theory level to determine the final global energy minimum structures (Ge et al., 2018; Zhao and Truhlar, 2008). To ensure that there are no imaginary frequencies, a frequency calculation was performed for each stationary point.

Previous studies have shown that M06-2X performs well in thermodynamic properties, non-covalent interactions (NCI), and equilibrium structures (Bork et al., 2014; Elm et al., 2012, 2013; Leverentz et al., 2013), and has been widely used in the calculation of the clusters containing amino acids recently (Wang et al., 2016; Elm et al., 2013; Ge et al., 2018). And the M06-2X theory level has good performance consistent with the MP2 theory level based on the similar results compared with MP2 (see Table S1, S2 in SI), which is an application of approximate integrals in ab initio theory with high accuracy, so we chose this method to obtain the structures and thermodynamic properties of the $(SA)_n$ $(Ala)_m$ and $(SA)_n$ $(Ser)_m$ (n, m = 1–4) clusters in this study.

We used the reduced density gradient (RDG) approach to clarify non-covalent interactions (NCI) (Johnson et al., 2010), and visualized it by the visual molecular dynamics (VMD) program (Humphrey et al., 1996), and analyzed the characteristics of bond critical points (BCPs) based on the "atoms in molecules" (AIM) theory of Bader (Bader, 1985; Carroll et al., 1988; Bone and Bader, 1996). All the above calculations were implemented by Multiwfn 3.0 (Lu and Chen, 2012).

### 2.2. Atmospheric cluster dynamics simulation

Thermodynamic data calculated at the M06-2X/6-311 + G (d, p) theory level was applied to the Atmospheric Cluster Dynamics Code (ACDC) kinetic model to perform cluster dynamics simulation and study the formation rates of the clusters in the atmosphere (McGrath et al., 2012; Kontkanen et al., 2018). ACDC investigates the temporal development of molecular cluster distribution by explicit solution of the birth-death equations, and the birth-death equations can be described as

$$\frac{dc_i}{dt} = \frac{1}{2}\sum_{j<i}\beta_{j,\,(i-j)}c_j c_{(i-j)} + \sum_j \gamma_{(i+j)\to i}c_{i+j} - \sum_j \beta_{i,\,j}c_i c_j - \frac{1}{2}\sum_{j<i}\gamma_{i\to j}c_i + Q_i - S_i$$

(1)

where $i$ and $j$ represent the clusters whose concentrations are given in the system, $\beta_{ij}$ represents the collision coefficient between clusters $i$ and

$j$, $c_i$ and $c_j$ represent the number densities of cluster $i$ and cluster $j$, $Q_i$ represents the additional source term of cluster $i$, and $S_i$ represents the possible loss term for cluster $i$. The collision coefficient $\beta_{ij}$ taken from the kinetic gas theory is written as (Ortega et al., 2012)

$$\beta_{ij} = \left(\frac{3}{4\pi}\right)^{1/6}\left(\frac{6k_bT}{m_i} + \frac{6k_bT}{m_j}\right)^{1/6}\left(V_i^{1/3} + V_j^{1/3}\right)^2 \quad (2)$$

where $k_b$ means the Boltzmann constant, $T$ means the temperature, $m_i$ and $V_i$ mean the mass and volume of cluster $i$, respectively. $\gamma_{i \to j}$ means the evaporation coefficient of a cluster $i$ divided into two smaller clusters including cluster $j$, and can be given as

$$\gamma_{(i+j) \to i} = \beta_{ij}\frac{c_i^e c_j^e}{c_{i+j}^e} = \beta_{ij}c_{ref}\,exp\left\{\frac{\triangle G_{i+j} - \triangle G_i - \triangle G_j}{k_bT}\right\} \quad (3)$$

where $c_j^e$ represents the equilibrium concentration of cluster $i$ , $\Delta G_i$ represents the free energy of formation of cluster $i$, and $c_{ref}$ represents the monomer concentration of the reference vapor. The formation rate is defined as the flux of clusters outside the system and can be calculated with

$$J = \sum_{i=0}^{m}\sum_{j=0}^{m}\sum_{k=0}^{n}\sum_{l=0}^{n}\beta_{ik,jl}\cdot c_{ik}\cdot c_{jl} \quad (4)$$
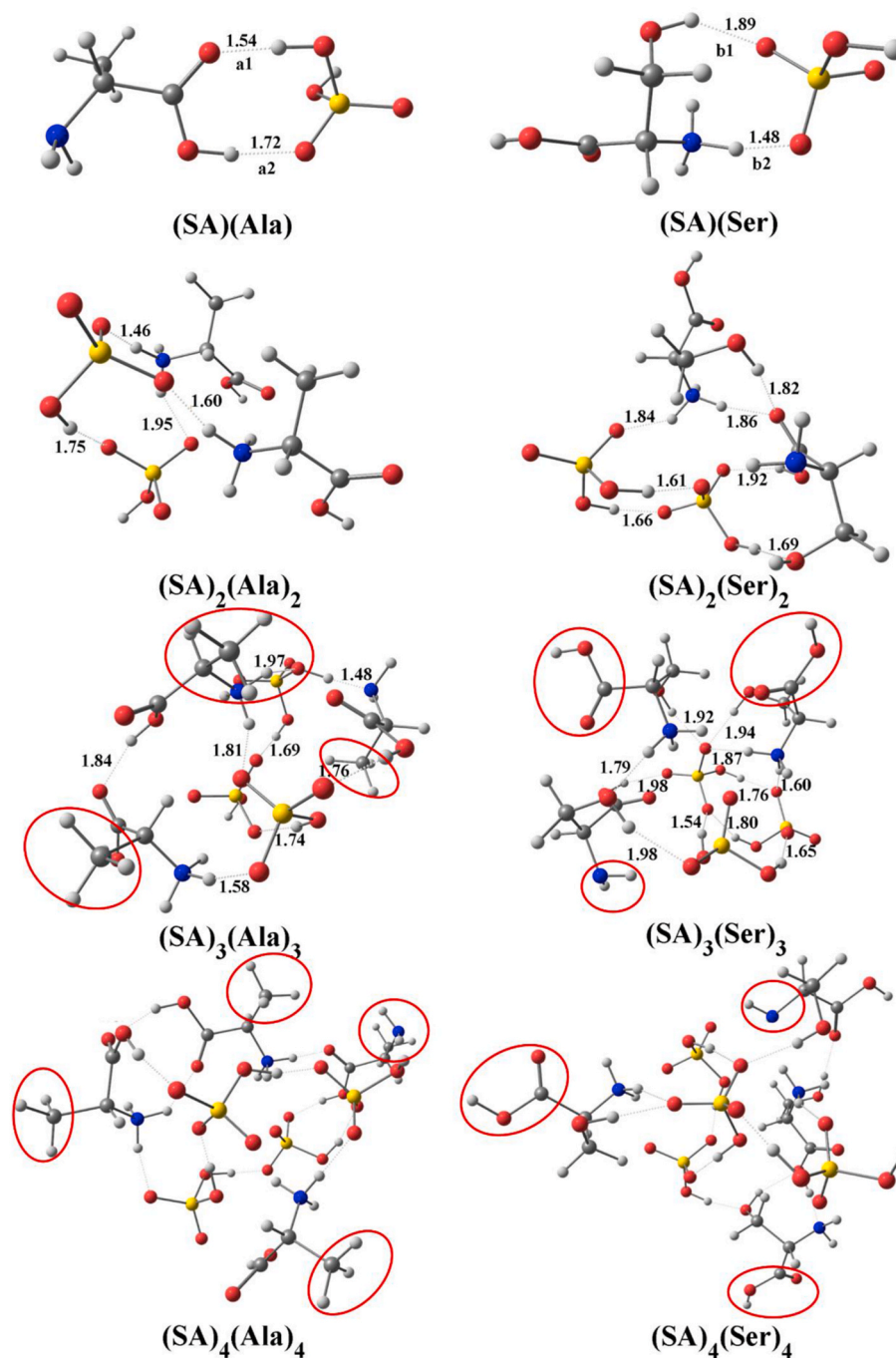


**Fig. 1.** The lowest-energy structures of the (SA)$_n$ (Ala)$_n$ (n = 1–4) and (SA)$_m$ (Ser)$_m$ (m = 1–4) clusters calculated at the M06-2X/6-311 + G (d, p) theory level. The lengths of hydrogen bond are given in Å. The red ellipses mark the un-bonded groups exposed at the edge of the clusters. (For interpretation of the references to colour in this figure legend, the reader is referred to the Web version of this article.)

where $m$ and $n$ correspond to the boundaries of the system, $i$ and $j$ correspond to the number of sulfuric acid molecules in the first and second cluster, respectively, and $k$ and $l$ correspond to the number of amino acid molecules, respectively. Ortega et al. proposed that clusters with more bases than acids are unstable (Ortega et al., 2012). Therefore, in the acid-base system simulation of McGrath et al. (2012), the restriction condition that the clusters contain at least one acid molecule was given. However, since both amino and carboxyl groups exist in amino acids, there is no need to add this restriction in our system, that is, the number of acid molecules in the formula can be increased from 0 (Zhao et al., 2019), the maximum number of sulfuric acid or amino

acid molecules in the cluster is 4. Meanwhile, we set different boundary sizes to study the contribution of clusters of different sizes to NPF (Zhao et al., 2019). Sulfuric acid concentrations range from $10^5$ to $10^9$ molecules cm$^{-3}$, depending on atmospheric observations and laboratory simulations of nucleation (Kulmala, 2003; Sipilä et al., 2010b). We use the enthalpy ($\Delta H$) and entropy ($\Delta S$) in place of the Gibbs free energy ($\Delta G = \Delta H - T\Delta S$) (McGrath et al., 2012), and the temperature range is set from 258.15 K to 298.15 K, corresponding to different ambient temperatures. Previous studies have pointed out that the atmospheric concentration of Ala and Ser in Beijing is at pptv level (Ren et al., 2018), so the concentration of amino acids is set to range from 1pptv to
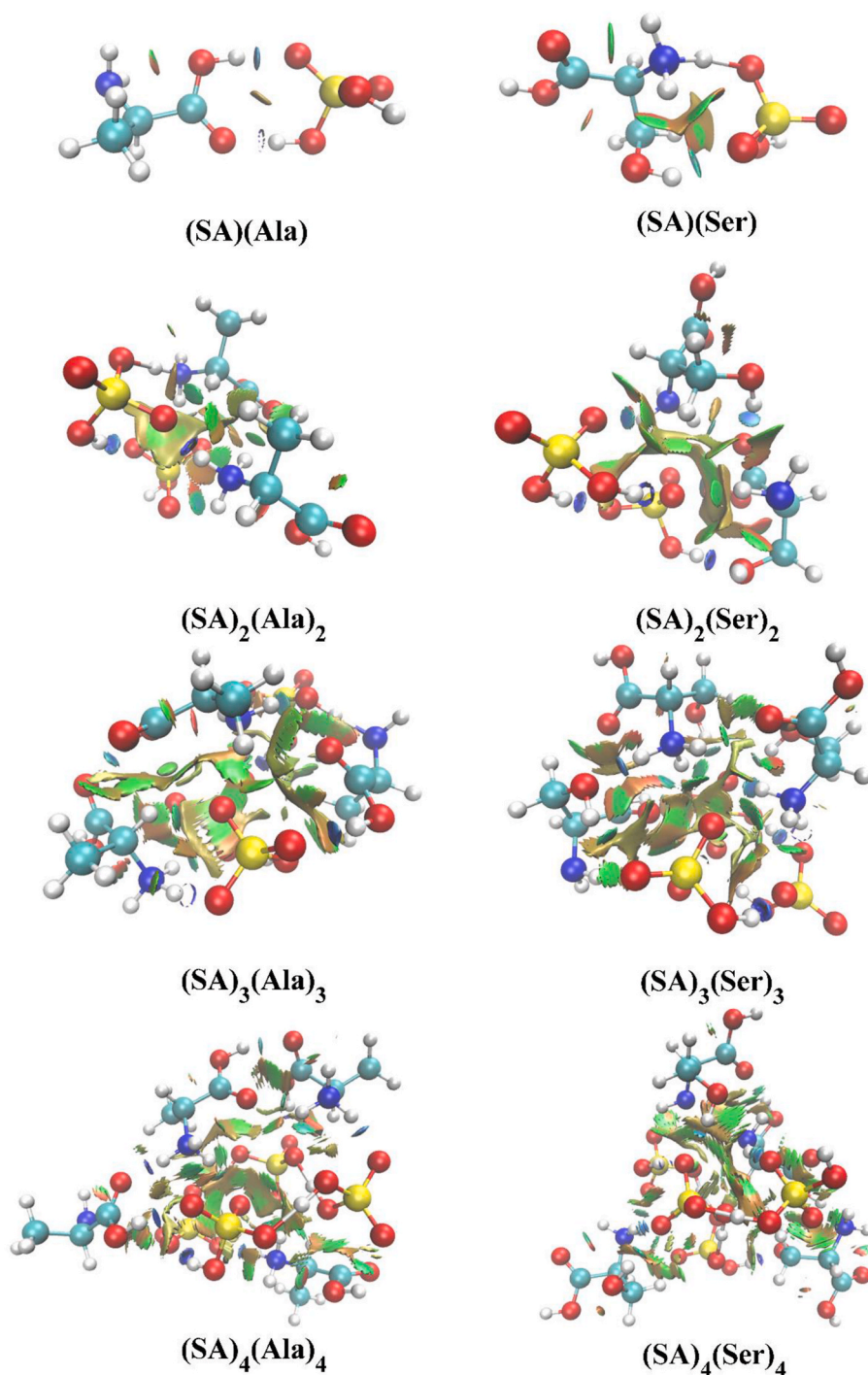


**Fig. 2.** Isosurfaces of the lowest-energy structures of the (SA)$_n$ (Ala)$_n$ (n = 1–4) and (SA)$_m$ (Ser)$_m$ (m = 1–4) clusters calculated at the M06-2X/6-311 + G (d, p) theory level.

100pptv.

## 3. Results and discussion

### 3.1. Structural analysis

All the structures of lowest Gibbs free energy of monomers and the (SA)$_n$ (Ala)$_m$ and (SA)$_n$ (Ser)$_m$ (n, m = 1–4) clusters are calculated at the M06-2X/6-311 + G (d, p) theory level and displayed in the Supporting Information Fig S1, Fig S2 and Fig S3. In order to discuss the structural differences between the two different amino acids in the process of forming clusters with sulfuric acid, we conduct structural analysis of (SA)$_n$ (Ala)$_n$ (n = 1–4) and (SA)$_m$ (Ser)$_m$ (m = 1–4) (see Fig. 1). The gradient isosurfaces provide abundant visualization information of non-covalent interactions while the blue area indicates strong attractive interaction, and red area indicates strong space steric effect (see Fig. 2). The disc formed by the isosurfaces between the hydrogen donor and the oxygen acceptor is characteristic of hydrogen bonds (Johnson et al., 2010). The "atoms in molecules" (AIM) theory of Bader is used to analyze the characteristics of bond critical points (BCPs) in the two-membered clusters (Bader, 1985; Carroll et al., 1988; Bone and Bader, 1996). The electron density (ρ), its Laplacian (Δ²ρ), the electronic kinetic energy density (G), the electronic potential energy density (V) and the electronic energy density (H) calculated by the Multiwfn program are given in Table 1 (Lu and Chen, 2012).

An Ala monomer has one amino group and one carboxyl group, and a Ser monomer has one more hydroxyl group than the Ala. For (SA) (Ala), there are two hydrogen bonds between the carboxyl group of the Ala and the sulfuric acid, with lengths of 1.54 and 1.72 Å, respectively. At the same time, it can be found in the isosurfaces that two blue discs form at the corresponding positions. However, for (SA) (Ser), the amino group and the hydroxyl group of the Ser participate in the formation of hydrogen bonds, while the carboxyl group doesn't. The length of the hydrogen bond between the hydroxyl group and the O atom in the sulfuric acid is 1.89 Å. Note that proton transfer occurs between the amino group of the Ser and the carboxyl group of the sulfuric acid, and a hydrogen bond with the length of 1.48 Å forms at the same time. The –G/V values corresponding to the hydrogen bonds formed by the oxygen atoms of sulfuric acid and the two amino acids (a2 and b1 in Table 1) are close to 1 and both Δ²ρ and H are positive, indicating that the interactions are non-covalent interactions and the hydrogen bonds are weak (Kim et al., 1994; Rozas et al., 2000). On the contrary, for the hydrogen bonds formed between hydrogen atoms of sulfuric acid and amino acids (a1 and b2 in Table 1), Δ²ρ are positive and H are negative, which are regarded as medium hydrogen bonds. And according to -G/V values, the interactions are partially covalent. Among them, the electronic density value of the hydrogen bond of length of 1.54 Å in (SA) (Ala) is 0.065 a.u., the electronic density value of the hydrogen bond of length of 1.48 Å in (SA) (Ser) is 0.082 a.u., and the larger the electronic density is, the stronger the hydrogen bond is (Gálvez et al., 2001). This indicates that the proton transfer does enhance the strength of the hydrogen bond (Stinson et al., 2016; Xu et al., 2017).

For (SA)$_2$(Ala)$_2$, there are four hydrogen bonds, two protons transfer between the carboxyl groups of sulfuric acid molecules and the amino groups of Ala molecules with the lengths of 1.60 and 1.46 Å, respectively. The other two hydrogen bonds are formed between sulfuric acid

and the Ala with lengths of 1.95 and 1.75 Å. In this cluster, the carboxyl groups of the Ala don't participate in the formation of hydrogen bonds, and no hydrogen bonds are formed between the two Ala molecules. The formations of hydrogen bonds of (SA)$_2$(Ser)$_2$ are more complicated compared with those of (SA)$_2$(Ala)$_2$. It can be found that three groups of the Ser in (SA)$_2$(Ser)$_2$ cluster are involved in the formation of hydrogen bonding, hydrogen bonds are formed between the two Ser molecules. In the (SA)$_2$(Ser)$_2$ cluster, a four-membered ring of -SA-SA-Ser-Ser-is formed by the bridged proton transfer.

As for (SA)$_n$ (Ala)$_n$ and (SA)$_m$ (Ser)$_m$ (n, m = 3–4) clusters, sulfuric acid molecules are located at the center, and Ala or Ser molecules interact with sulfuric acids to form hydrogen bonds and grow outward in general. In this process, proton transfer and the formations of hydrogen bonds between Ala molecules or Ser molecules occur frequently as well. For (SA)$_n$ (Ala)$_n$ (n = 3–4), the carboxyl and amino groups of Ala molecules mostly form hydrogen bonds with sulfuric acid at the center of the cluster, while the methyl groups are exposed at the edge of the cluster. For (SA)$_m$ (Ser)$_m$ (m = 3–4), the hydroxyl groups of Ser molecules are more involved in the formation of hydrogen bonds at the center of the cluster, while the carboxyl and amino groups are more exposed at the edge of the cluster.

In conclusion, for two-membered and four-membered clusters, the introduction of the Ser's hydroxyl groups provides more hydrogen bonding sites and causes a synergistic effect between hydroxyl, amino and carboxyl groups, resulting in more functional groups participated in the formation of hydrogen bonds, promoting proton transfer between the amino and sulfuric acids occur earlier, and making the Ser more conducive to the formation of hydrogen bonds than the Ala in small clusters. In addition, the strong bridged proton transfer in (SA)$_m$ (Ser)$_m$ (m = 1–2) clusters enhances the strength of hydrogen bonds, making the structures of the clusters more stable. For six-membered and eight-membered clusters, in general, the formation of hydrogen bonds in the clusters depend mainly on sulfuric acid molecules. For (SA)$_m$ (Ser)$_m$ (m = 3–4), the synergistic effect caused by the Ser's hydroxyl groups will gradually decrease. On the contrary, the introduction of hydroxyl groups hinders the formation of hydrogen bonds between the carboxyl and amino groups of Ser molecules and sulfuric acid molecules, that is the steric effect, resulting in more un-bonded carboxyl and amino groups exposed at the edge of the cluster, making the structures of (SA)$_m$ (Ser)$_m$ cluster less stable than those of (SA)$_n$ (Ala)$_n$ (n, m = 3–4, n = m).

### 3.2. Thermochemical analysis

The calculation results of the relative zero-point correction energy ΔE (0 K), the intermolecular enthalpy ΔH (298.15 K) and the Gibbs free energy ΔG (298.15 K) of (SA)$_n$ (Ala)$_m$ and (SA)$_n$ (Ser)$_m$ (n, m = 1–4) clusters at the M06-2X/6-311 + G (d, p) theory level are given in Table 2 and Table 3, respectively. In each Table, the values are calculated with

$$\Delta E_{(SA)_n(X)_m} = E_{(SA)_n(X)_m} - nE_{SA} - mE_X \quad (5)$$

$$\Delta H_{(SA)_n(X)_m} = H_{(SA)_n(X)_m} - nH_{SA} - mH_X \quad (6)$$

$$\Delta G_{(SA)_n(X)_m} = G_{(SA)_n(X)_m} - nG_{SA} - mG_X \quad (7)$$

where X represents Ala or Ser.

According to Tables 2 and 3, all the ΔG values are negative,

**Table 1**
Lengths of hydrogen bonds and topological parameters of the BCPs in (SA) (Ala) and (SA) (Ser) clusters at the M06-2X/6-311 + G (d, p) theory level. The labels are given in Fig. 1.

| Clusters | Labels | L/Å | ρ/a.u. | G/a.u. | V/a.u. | H/a.u. | Δ²ρ/a.u. | -G/V |
|---|---|---|---|---|---|---|---|---|
| **(SA) (Ala)** | a1 | 1.54 | 0.065 | 0.055 | −0.072 | −0.016 | 0.156 | 0.764 |
| | a2 | 1.72 | 0.037 | 0.036 | −0.036 | 0.000 | 0.141 | 1.000 |
| **(SA) (Ser)** | b1 | 1.89 | 0.028 | 0.026 | −0.025 | 0.002 | 0.112 | 1.040 |
| | b2 | 1.48 | 0.082 | 0.065 | −0.094 | −0.029 | 0.143 | 0.691 |

**Table 2**

The calculation results of $\Delta E$, $\Delta H$ and $\Delta G$ of $(SA)_n (Ala)_m$ (n, m = 1–4) clusters at the M06-2X/6-311 + G (d, p) theory level. The energies are in kcal mol$^{-1}$.

| Reactions | $\Delta E$ (0 K) | $\Delta H$ (298.15 K) | $\Delta G$ (298.15 K) |
|---|---|---|---|
| SA + Ala ↔ (SA) (Ala) | −19.6 | −20.2 | −8.5 |
| SA+2Ala ↔ (SA) (Ala)$_2$ | −39.5 | −39.8 | −14.3 |
| SA+3Ala ↔ (SA) (Ala)$_3$ | −57.5 | −57.7 | −20.0 |
| SA+4Ala ↔ (SA) (Ala)$_4$ | −72.7 | −72.6 | −21.8 |
| 2SA + Ala ↔ (SA)$_2$(Ala) | −46.0 | −46.6 | −20.9 |
| 2SA+2Ala ↔ (SA)$_2$(Ala)$_2$ | −74.1 | −74.3 | −37.0 |
| 2SA+3Ala ↔ (SA)$_2$(Ala)$_3$ | −95.1 | −95.6 | −42.7 |
| 2SA+4Ala ↔ (SA)$_2$(Ala)$_4$ | −116.4 | −116.4 | −52.6 |
| 3SA + Ala ↔ (SA)$_3$(Ala) | −72.9 | −73.9 | −33.3 |
| 3SA+2Ala ↔ (SA)$_3$(Ala)$_2$ | −101.8 | −103.3 | −49.4 |
| 3SA+3Ala ↔ (SA)$_3$(Ala)$_3$ | −136.3 | −137.2 | −69.7 |
| 3SA+4Ala ↔ (SA)$_3$(Ala)$_4$ | −152.1 | −152.5 | −73.6 |
| 4SA + Ala ↔ (SA)$_4$(Ala) | −100.2 | −100.8 | −48.5 |
| 4SA+2Ala ↔ (SA)$_4$(Ala)$_2$ | −118.2 | −119.2 | −53.2 |
| 4SA+3Ala ↔ (SA)$_4$(Ala)$_3$ | −166.4 | −167.3 | −87.2 |
| 4SA+4Ala ↔ (SA)$_4$(Ala)$_4$ | −197.2 | −198.5 | −103.3 |

**Table 3**

The calculation results of $\Delta E$, $\Delta H$ and $\Delta G$ of $(SA)_n (Ser)_m$ (n, m = 1–4) clusters at the M06-2X/6-311 + G (d, p) theory level. The energies are in kcal mol$^{-1}$.

| Reactions | $\Delta E$ (0 K) | $\Delta H$ (298.15 K) | $\Delta G$ (298.15 K) |
|---|---|---|---|
| SA + Ser ↔ (SA) (Ser) | −24.2 | −24.3 | −12.2 |
| SA+2Ser ↔ (SA) (Ser)$_2$ | −47.3 | −47.3 | −22.2 |
| SA+3Ser ↔ (SA) (Ser)$_3$ | −69.0 | −69.3 | −29.9 |
| SA+4Ser ↔ (SA) (Ser)$_4$ | −86.5 | −86.6 | −34.5 |
| 2SA + Ser ↔ (SA)$_2$(Ser) | −55.7 | −55.9 | −31.2 |
| 2SA+2Ser ↔ (SA)$_2$(Ser)$_2$ | −74.5 | −74.9 | −36.2 |
| 2SA+3Ser ↔ (SA)$_2$(Ser)$_3$ | −101.4 | −101.6 | −50.2 |
| 2SA+4Ser ↔ (SA)$_2$(Ser)$_4$ | −124.5 | −124.9 | −60.1 |
| 3SA + Ser ↔ (SA)$_3$(Ser) | −81.5 | −81.7 | −44.6 |
| 3SA+2Ser ↔ (SA)$_3$(Ser)$_2$ | −108.8 | −109.1 | −58.8 |
| 3SA+3Ser ↔ (SA)$_3$(Ser)$_3$ | −133.9 | −134.7 | −66.9 |
| 3SA+4Ser ↔ (SA)$_3$(Ser)$_4$ | −163.1 | −163.7 | −83.1 |
| 4SA + Ser ↔ (SA)$_4$(Ser) | −103.4 | −103.4 | −53.3 |
| 4SA+2Ser ↔ (SA)$_4$(Ser)$_2$ | −136.4 | −136.5 | −72.2 |
| 4SA+3Ser ↔ (SA)$_4$(Ser)$_3$ | −162.2 | −163.1 | −83.3 |
| 4SA+4Ser ↔ (SA)$_4$(Ser)$_4$ | −182.9 | −183.4 | −90.8 |

indicating all the reactions in both tables can occur spontaneously in the atmosphere. For $(SA) (Ala)_m$ (m = 1–4), the $\Delta G$ values are −8.5, −14.3, −20.0 and −21.8 kcal mol$^{-1}$, respectively. For $(SA) (Ser)_m$ (m = 1–4), the $\Delta G$ values are −12.2, −22.2, −29.9 and −34.5 kcal mol$^{-1}$, respectively. Hence, for clusters with the same number of molecules, the $\Delta G$ values of $(SA) (Ser)_m$ are smaller than those of $(SA) (Ala)_m$ (m = 1–4), indicating the $(SA) (Ser)_m$ cluster are more stable than $(SA) (Ala)_m$ (m = 1–4). For $(SA)_2(Ala)_m$ and $(SA)_2(Ser)_m$ (m = 1–4), almost all the $\Delta G$ values of $(SA)_2(Ser)_m$ are smaller than those of $(SA)_2(Ala)_m$, except for $(SA)_2(Ala)_2$ and $(SA)_2(Ser)_2$, with the values of −37.0 and −36. 2 kcal mol$^{-1}$, respectively. For $(SA)_n (Ala)_m$ and $(SA)_n (Ser)_m$ (n, m = 3–4), there are more cases where the relationship of $\Delta G$ does not conform to the above rule. This possibly indicates that the Ser can form more stable clusters with sulfuric acids compared with the Ala in small clusters due to the synergistic effect between hydroxyl, amino and carboxyl groups. However, with the increase of cluster's size, the effect of the synergistic effect will gradually decrease. In large clusters, the introduction of hydroxyl groups makes more carboxyl groups and amino groups exposed at the edge of the clusters, unable to form bonds with sulfuric acid molecules, which in turn reduces the stability of the cluster.

Based on above results, we can find that with the increase of molecular number in the clusters, the value of $\Delta G$ decreases gradually in general, which seems to indicate that the cluster can grow spontaneously in the atmosphere. Especially for $(SA) (Ala)_m$ and $(SA) (Ser)_m$ (m = 1–4), the decreasing range of $\Delta G$ also decreases gradually with the increase of molecular number, and when adding an Ser molecule, the decreasing range of $\Delta G$ is larger than that of adding an Ala molecule.

This can be validated by the above analysis that the Ser is more conducive to the formation of the clusters than the Ala in small clusters. However, as the sizes of the clusters increase, the steric effect has a negative feedback effect on the stability of the structures.

Heatmaps of the $\Delta G$ are given in Fig. 3 as an intuitive description of how the $\Delta G$ value changes with the increasing number of sulfuric acid molecules and amino acid molecules. To be specific, the $\Delta G$ values of $(SA)_n (Ala)_n$ (n = 1–4) are −8.5, −37.0, −69.7 and −103.3 kcal mol$^{-1}$, respectively, while the $\Delta G$ values of $(SA)_m (Ser)_m$ (m = 1–4) are −12.2, −36.2, −66.9 and −90.8 kcal mol$^{-1}$, respectively. It can be concluded that for small clusters, due to the synergistic effect, the structures of SA-Ser system are more stable than those of SA-Ala system, while for large clusters, the steric effect makes SA-Ala system more stable than SA-Ser system. As shown in Fig. 3, the $\Delta G$ of the structure on the diagonal of the heat map seems to be more negative, which indicates that the clusters may grow diagonally as well. This may indicates that the SA-Ser/SA-Ala systems have a trend of low free energy barrier along the diagonal similar to the acid-base system (Schobesberger et al., 2013; Xu et al., 2020).

### 3.3. Atmospheric relevance

In this part, $(SA)_n (Ala)_n$ and $(SA)_m (Ser)_m$ (n, m = 1–4) clusters on the diagonal of heatmaps of $\Delta G$ are selected to calculate the formation rates by ACDC (McGrath et al., 2012) and perform atmospheric relevance analysis. The method of controlling variables is used to set different conditions, discussing the effect of temperature and concentration on the formation rate in the two types of clusters with different size.

### 3.3.1. Formation rates vs the concentration of sulfuric acid

Most atmospheric observation results indicate nucleation occurs when the concentration of sulfuric acid is slightly higher than $10^5$ molecules cm$^{-3}$, which have been successfully simulated under atmospheric laboratory conditions (Kulmala, 2003; Sipilä et al., 2010b; Birmili et al., 2000; Kuang, 2008; Weber, 1996, 1999; Berndt et al., 2005; Nieminen et al., 2009). To discuss the relationship of the formation rates of the clusters on the diagonal, the formation rates of the $(SA)_n (Ala)_n$ and $(SA)_m (Ser)_m$ (n, m = 1–4) clusters at the concentration range of sulfuric acid of $10^5$ to $10^9$ molecules cm$^{-3}$ are described in Fig. 4.

As shown in Fig. 4, we can find that under the same conditions, when the concentration of sulfuric acid increases, the formation rates of the clusters will gradually increase. Comparing the formation rates of $(SA)_n (Ala)_n$ (n = 1–4) at the same concentration of sulfuric acid, we can find the ranking of the formation rates of the four clusters is as follows: $(SA) (Ala) > (SA)_2(Ala)_2 > (SA)_3(Ala)_3 > (SA)_4(Ala)_4$, the formation rate gradually decreases with the increase of cluster's size. When the sulfuric acid concentration varies from $10^5$ to $10^9$ molecules cm$^{-3}$, the formation rates of $(SA) (Ala)$, $(SA)_2(Ala)_2$, $(SA)_3(Ala)_3$ and $(SA)_4(Ala)_4$ increase by 4, 8, 10 and 12 orders of magnitude, respectively. And in this process, the ranking of the increases of the formation rates of the four clusters is as follows: $(SA) (Ala) < (SA)_2(Ala)_2 < (SA)_3(Ala)_3 < (SA)_4(Ala)_4$. It can be speculated that as the sulfuric acid concentration increases, the difference between the formation rates of four clusters will decrease. This may be due to that the formation rates of large clusters are much more depended on the concentration of sulfuric acid than those of small clusters. And the analysis results for $(SA)_m (Ser)_m$ (m = 1–4) clusters in this part are the same as those of $(SA)_n (Ala)_n$ (n = 1–4) clusters.

For two-membered and four-membered clusters, when the sulfuric acid concentration is $10^5$ molecules cm$^{-3}$, the formation rates of $(SA) (Ala)$, $(SA) (Ser)$, $(SA)_2(Ala)_2$ and $(SA)_2(Ser)_2$ are $10^{-1}$, $10^2$, $10^{-6}$ and $10^{-5}$ cm$^{-3}$ s$^{-1}$, respectively. And when the sulfuric acid concentration is $10^9$ molecules cm$^{-3}$, the formation rates of $(SA) (Ala)$, $(SA) (Ser)$, $(SA)_2(Ala)_2$ and $(SA)_2(Ser)_2$ are $10^3$, $10^7$, $10^2$, and $10^5$ cm$^{-3}$ s$^{-1}$, respectively. This shows that under the same conditions, the formation rates of $(SA)_m (Ser)_m$ (m = 1–2) are higher than that of $(SA)_n (Ala)_n$ (n =

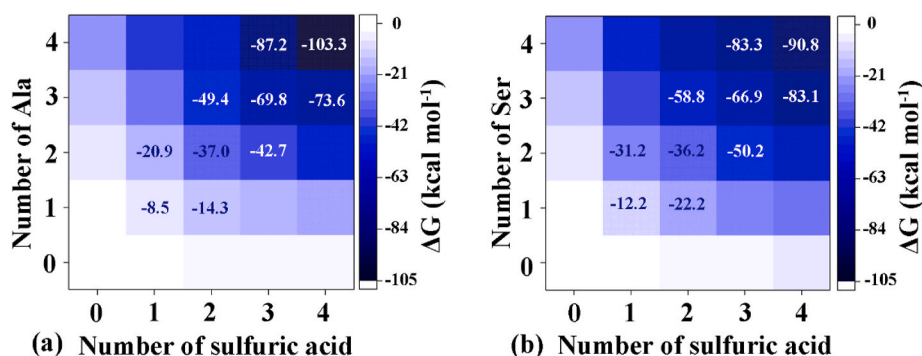**Fig. 3.** Heatmaps of the $\Delta G$ on the SA–Ala and SA–Ser grid at 298.15 K: (a) $(SA)_n (Ala)_n$ (n = 1–4), (b) $(SA)_m (Ser)_m$ (m = 1–4).



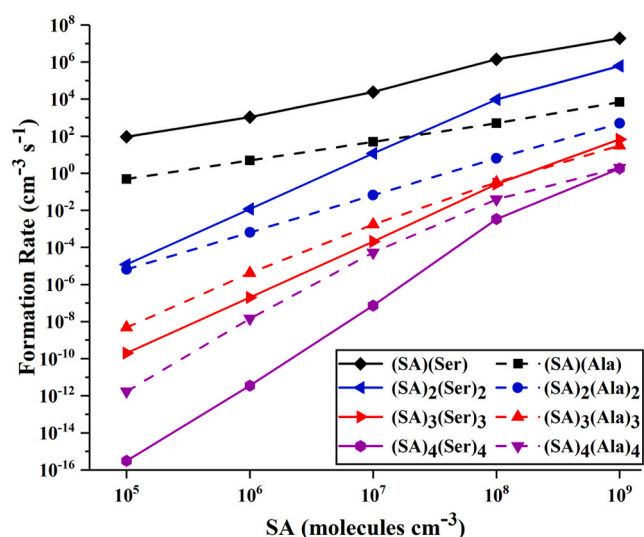**Fig. 4.** The cluster formation rate (cm$^{-3}$ s$^{-1}$) as a function of the concentration of sulfuric acid for different clusters: the black solid line represents (SA) (Ser), the blue solid line represents $(SA)_2(Ser)_2$, the red solid line represents $(SA)_3(Ser)_3$, the purple solid line represents $(SA)_4(Ser)_4$, the black dotted line represents (SA) (Ala), the blue dotted line represents $(SA)_2(Ala)_2$, the red dotted line represents $(SA)_3(Ala)_3$, the purple dotted line represents $(SA)_4(Ala)_4$. The concentration of sulfuric acid ranges 10$^5$ to 10$^9$ molecules cm$^{-3}$, [amino acid] = 10 pptv, 298.15 K. (For interpretation of the references to colour in this figure legend, the reader is referred to the Web version of this article.)

1–2), And this can indicate that the synergistic effect caused by hydroxyl groups and the stronger bridged proton transfer make the Ser more favorable for nucleation than the Ala in small clusters.

For six-membered and eight-membered clusters, when the sulfuric acid concentration is 10$^5$ molecules cm$^{-3}$, the formation rates of $(SA)_3(Ala)_3$, $(SA)_3(Ser)_3$, $(SA)_4(Ala)_4$ and $(SA)_4(Ser)_4$ are 10$^{-9}$, 10$^{-10}$, 10$^{-12}$ and 10$^{-16}$ cm$^{-3}$ s$^{-1}$, respectively. And when the sulfuric acid concentration is 10$^9$ molecules cm$^{-3}$, the formation rates of $(SA)_3(Ala)_3$, $(SA)_3(Ser)_3$, $(SA)_4(Ala)_4$ and $(SA)_4(Ser)_4$ are 10$^1$, 10$^1$, 10$^0$ and 10$^0$ cm$^{-3}$ s$^{-1}$, respectively. It can be seen that when the concentration of sulfuric acid is 10$^5$ molecules cm$^{-3}$, the formation rates of $(SA)_n (Ala)_n$ (n = 3–4) are higher than those of $(SA)_m (Ser)_m$ (n = 3–4). This could be explained by that the steric effect, reduces the stability of the cluster's structure. When the concentration of sulfuric acid is 10$^9$ molecules cm$^{-3}$, the formation rates of $(SA)_n (Ala)_n$ (n = 3–4) and $(SA)_m (Ser)_m$ (n = 3–4) are on the same order of magnitude. This shows that for clusters with more sulfuric acid molecules, the effect of the steric effect on clusters could be ignored and the formation rate of clusters mainly depend on the concentration of sulfuric acid. Therefore, at high sulfuric acid concentrations, there are no obvious difference in the formation rates of $(SA)_n$

$(Ala)_n$ (n = 3–4) and $(SA)_m (Ser)_m$ (m = 3–4).

### 3.3.2. Formation rates vs the concentration of amino acid

Ren et al. reported that the high annual average concentration of amino acids in the Beijing area may be related to biological or bacterial effects, because viruses, bacteria, spores and pollen play an important role in particles containing cell proteins (Feltracco et al., 2019; Matos et al., 2016; Mandalakis et al., 2011). The chemical analysis of the samples obtained by sampling and filtering the ambient air shows that the concentrations of Ser and Ala in Beijing urban aerosol range at pptv level (Ren et al., 2018), the concentrations of Ala and Ser are set at 1, 10 and 100 pptv to discuss the effect of the concentration of amino acid on cluster formation rate. Fig. 5 shows the formation rates curves of the $(SA)_n (Ala)_n$ and $(SA)_m (Ser)_m$ (n, m = 1–4) clusters at the concentration range of sulfuric acid from 10$^5$ to 10$^9$ molecules cm$^{-3}$ and the concentration range of Ala and Ser from 1 to 100pptv.

As shown in Fig. 5, we can find that under the same conditions, when the concentrations of amino acid increase, the formation rates of clusters will gradually increase. Take $(SA)_n (Ala)_n$ (n = 1–2) clusters for example, when the sulfuric acid concentration is 10$^5$ molecules cm$^{-3}$, the concentration of Ala is set to 1, 10 and 100pptv, the formation rates of (SA) (Ala) are 10$^{-3}$, 10$^{-1}$ and 10$^1$ cm$^{-3}$ s$^{-1}$ respectively, the formation rates of $(SA)_2(Ala)_2$ are 10$^{-9}$, 10$^{-6}$ and 10$^{-3}$ cm$^{-3}$ s$^{-1}$ respectively. As concentration of sulfuric acid increases, the increase of formation rates of $(SA)_n (Ala)_n$ (n = 1–2) promoted by Ala's concentration are the same, and the corresponding formation rate curves at three concentrations of amino acid in Fig. 5 are almost parallel.

### 3.3.3. Temperature dependence of formation rates

To discuss the effect of temperature on the formation rate of $(SA)_n$ $(Ala)_n$ and $(SA)_m (Ser)_m$ (n, m = 1–2, n = m) clusters, three temperature points were considered at 258.15, 278.15 and 298.15 K, respectively. As shown in Fig. 6, the formation rate curves of the $(SA)_n (Ala)_n$ and $(SA)_m$ $(Ser)_m$ (n, m = 1–4, n = m) clusters at the concentration range of sulfuric acid from 10$^5$ to 10$^9$ molecules cm$^{-3}$, the concentrations of Ala and Ser are set at 10pptv.

Comparing the formation rates of $(SA)_n (Ala)_n$ and $(SA)_m (Ser)_m$ (n, m = 1–4) at the same concentration and different temperature conditions, we can find the ranking of the formation rates of the same cluster under three temperature conditions is as follows: 258.15 K > 278.15 K > 298.15 K, the formation rates of clusters gradually decrease with the increase of temperature, which is similar to the relationship of temperature dependence of $H_2SO_4$–$NH_4$ experimental results reported by Dunne et al. (2016).

For most cases, at lower concentration of sulfuric acid, the effect of increasing temperature on the formation rates of clusters is significantly greater than that at higher concentration of sulfuric acid. For example, when the sulfuric acid concentration is 10$^5$ molecules cm$^{-3}$ and temperature is 258.15, 278.15 and 298.15 K respectively, the formation rates of $(SA)_4(Ser)_4$ are 4.11 × 10$^{-6}$, 7.70 × 10$^{-10}$ and 3.08 × 10$^{-16}$
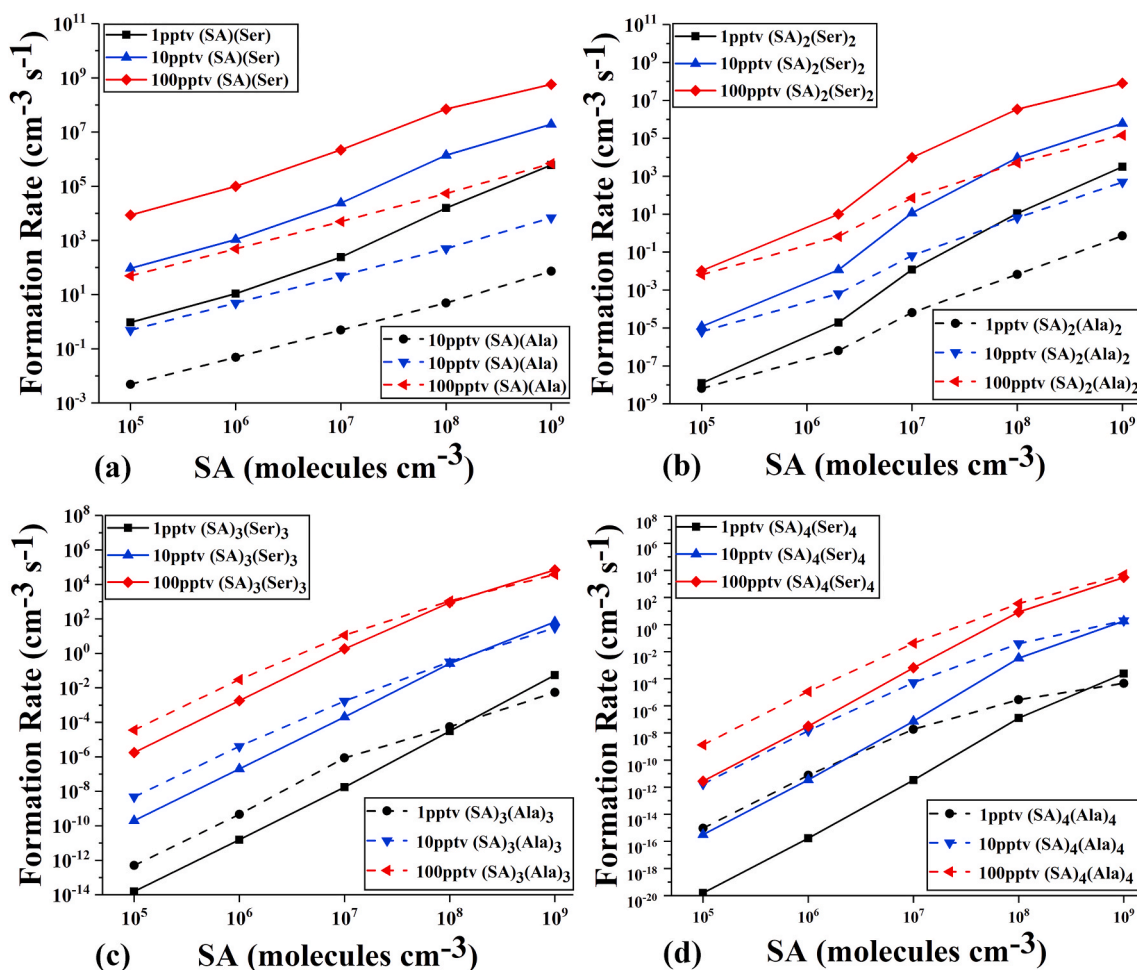
**Fig. 5.** The cluster formation rate (cm$^{-3}$ s$^{-1}$) as a function of the concentration of amino acid for different clusters: (a) (SA) (Ala) and (SA) (Ser), (b) (SA)$_2$(Ala)$_2$ and (SA)$_2$(Ser)$_2$, (c) (SA)$_3$(Ala)$_3$ and (SA)$_3$(Ser)$_3$, (d) (SA)$_4$(Ala)$_4$ and (SA)$_4$(Ser)$_4$. Black represents [amino acid] = 1 pptv, blue represents [amino acid] = 10 pptv, red represents [amino acid] = 100 pptv, the dotted lines represent SA-Ala system, the solid lines represent SA-Ser system. The concentration of sulfuric acid ranges $10^5$ to $10^9$ molecules cm$^{-3}$, 298.15 K. (For interpretation of the references to colour in this figure legend, the reader is referred to the Web version of this article.)

cm$^{-3}$ s$^{-1}$ respectively, that is, the formation rate of (SA)$_4$(Ser)$_4$ decreased by 10 orders of magnitude when temperature increased by 40 K. However, when the sulfuric acid concentration is $10^9$ molecules cm$^{-3}$, the formation rate of (SA)$_4$(Ser)$_4$ decreased by 5 orders of magnitude when temperature increased by 40 K. This may be related to the contribution of temperature effect on the formation rates would be reduces as the increasing of the concentration of sulfuric acid.

For (SA) (Ala) and (SA) (Ser), when the sulfuric acid concentration is $10^9$ molecules cm$^{-3}$ and temperature is 258.15, 278.15 and 298.15 K respectively, the formation rates of (SA) (Ala) are $2.47 \times 10^7$, $4.36 \times 10^5$ and $6.91 \times 10^3$ cm$^{-3}$ s$^{-1}$ respectively, the formation rates of (SA) (Ser) are $1.31 \times 10^8$, $8.01 \times 10^7$ and $1.92 \times 10^7$ cm$^{-3}$ s$^{-1}$ respectively. It can be seen that the formation rate of (SA) (Ala) decreases by 2 orders of magnitude with every 20 K increase in temperature, while the formation rates of (SA) (Ser) are basically an order of magnitude under adjacent condition. This seems to indicate the same temperature change has smaller effect on the formation rate of (SA) (Ser) than that of (SA) (Ala), and a similar conclusion can be obtained for (SA)$_2$(Ala)$_2$ and (SA)$_2$(Ser)$_2$. The temperature dependence of (SA)$_m$ (Ser)$_m$ is less than that of (SA)$_n$ (Ala)$_n$ (n, m = 1–2, n = m), which may be explained by the synergistic effect and the enhancement of the stability of clusters by the strong bridged proton transfer. However for large clusters, temperature and the concentrations of sulfuric acid and amino acid have a greater influence on the formation rates than amino acid's structure, and temperature dependence of the two systems is not significantly different.

## 4. Conclusions

In this study, the lowest energy structures and thermodynamic analysis of the (SA)$_n$ (Ala)$_m$ and (SA)$_n$ (Ser)$_m$ (n, m = 1–4) clusters are calculated at the M06-2X/6-311 + G (d, p) theory level. The (SA)$_n$ (Ala)$_n$ and (SA)$_m$ (Ser)$_m$ (n, m = 1–4, m = n) clusters are selected for atmospheric relevance analysis.

Analysis results based on structural and thermochemical data show that in small clusters, the introduction of the Ser's hydroxyl groups causes a synergistic effect between hydroxyl, amino and carboxyl groups, resulting in more functional groups participate in the formation of hydrogen bonds, promoting proton transfer and improving the stability of the clusters. With the increase of cluster's size, the synergistic effect will gradually decrease, the introduction of the Ser's hydroxyl groups will interfere with the bonding between amino and carboxyl groups of Ser and sulfuric acid molecules, resulting in the steric effect, which leads to the decrease of the stability of the clusters.

Atmospheric relevance studies have shown that as the concentration of sulfuric acid increases, the formation rates of clusters will gradually increase. Under the same conditions, the formation rates of (SA)$_m$ (Ser)$_m$ are higher than that of (SA)$_n$ (Ala)$_n$ (n, m = 1–2, n = m), while the formation rates of (SA)$_m$ (Ser)$_m$ are slightly lower than those of (SA)$_n$ (Ala)$_n$ (n, m = 3–4), indicating the synergistic effect improves the stability of small clusters, while the steric effect reduces the stability of large clusters. As the concentration of amino acid increases, the
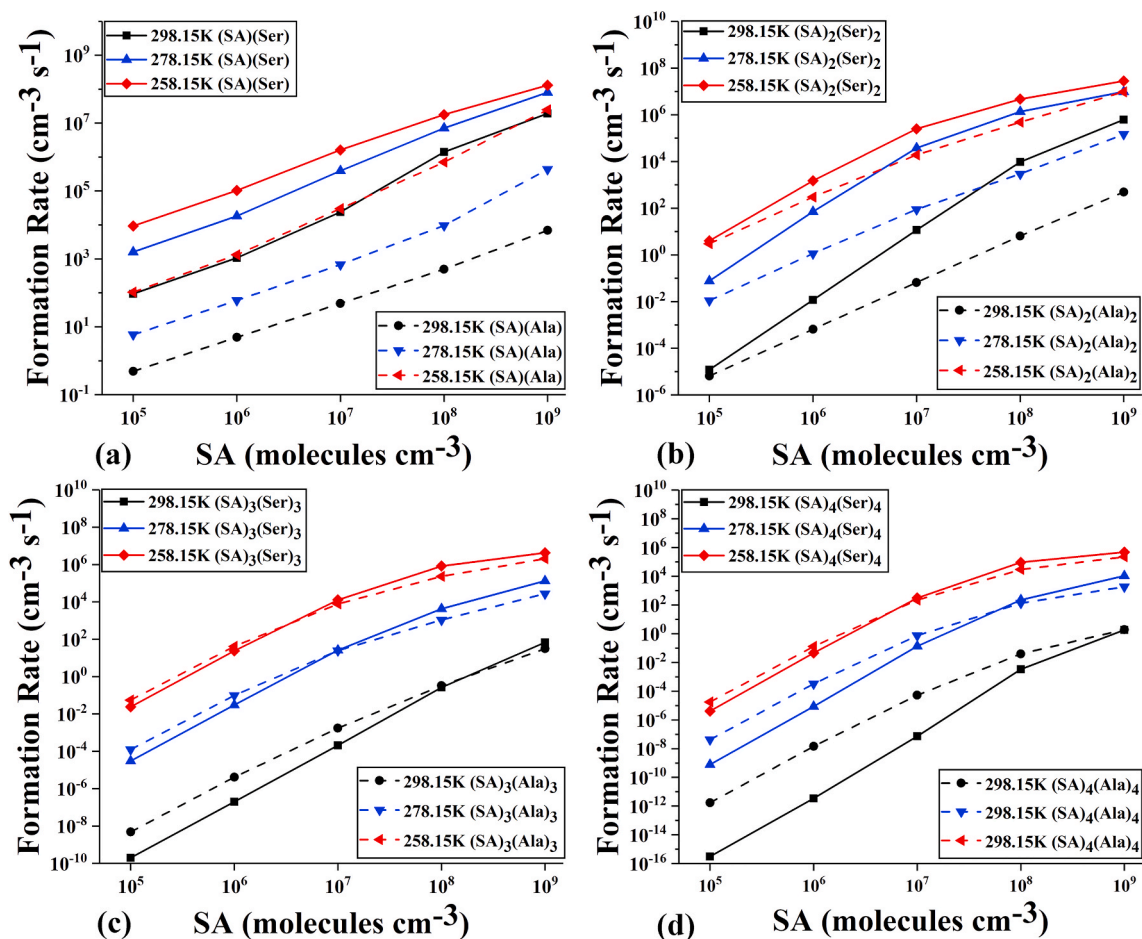
**Fig. 6.** The cluster formation rate (cm$^{-3}$ s$^{-1}$) as a function of temperature for different clusters: (a) (SA) (Ala) and (SA) (Ser), (b) (SA)$_2$(Ala)$_2$ and (SA)$_2$(Ser)$_2$, (c) (SA)$_3$(Ala)$_3$ and (SA)$_3$(Ser)$_3$, (d) (SA)$_4$(Ala)$_4$ and (SA)$_4$(Ser)$_4$. Black represents 298.15 K, blue represents 278.15 K, red represents 258.15 K, the dotted lines represent SA-Ala system, the solid lines represent SA-Ser system. The concentration of sulfuric acid ranges 10$^5$ to 10$^9$ molecules cm$^{-3}$, [amino acid] = 10 pptv. (For interpretation of the references to colour in this figure legend, the reader is referred to the Web version of this article.)

formation rates of clusters will gradually increase and the increase of formation rates promoted by amino acid's concentration is the same. Temperature dependence analysis of the formation rates shows that the lower the temperature, the higher the formation rates. At lower concentration of sulfuric acid, the effect of increasing temperature on the formation rates is significantly greater than that at higher concentration of sulfuric acid. It is worth noting that the temperature dependence of (SA)$_m$ (Ser)$_m$ is less than that of (SA)$_n$ (Ala)$_n$ (n, m = 1–2, n = m), indicating the structures of SA-Ser system are more stable than those of SA-Ala system in small cluster, while in large clusters, temperature and the concentrations of sulfuric acid and amino acid have a greater influence on the formation rates than amino acid's structure, and the temperature dependence of the two systems is not significantly different.

Our study shows that both Ala and Ser can form clusters with sulfuric acid, but the nucleation mechanism of the two amino acids shows obvious differences, which provides a starting point for further studies on the role of different amino acids with different functional groups in NPF. In addition, a more diversified system involving sulfuric acid and amino acids needs further study.

**CRediT authorship contribution statement**

**Hui Cao:** Conceptualization, Methodology, Data curation, Writing - original draft, Writing - review & editing. **Yi-Rong Liu:** Software, Investigation, Visualization. **Teng Huang:** Resources. **Shuai Jiang:** Formal analysis, Data curation. **Zi-Hang Wang:** Writing - review &

editing. **Ying Liu:** Visualization. **Ya-Juan Feng:** Methodology, Validation, Formal analysis, Writing - review & editing. **Wei Huang:** Methodology, Software, Supervision, Project administration, Funding acquisition.

**Declaration of competing interest**

The authors declare that they have no known competing financial interests or personal relationships that could have appeared to influence the work reported in this paper.

**Appendix A. Supplementary data**

Supplementary data to this article can be found online at https://doi.org/10.1016/j.atmosenv.2020.118139.

# References

Aber, J.D., et al., 1989. Nitrogen saturation in northern forest ecosystems. Bioscience 39 (6), 378-286.

Al Natsheh, A., et al., 2004. Sulfuric acid and sulfuric acid hydrates in the gas Phase: A DFT investigation. J. Phys. Chem. A 108 (41), 8914–8929.

Andreae, M.O., Crutzen, P.J., 1997. Atmospheric aerosols: biogeochemical sources and role in atmospheric chemistry. Science 276 (5315), 1052–1058.

Bader, R.F., 1985. Atoms in molecules. Acc. Chem. Res. 18 (1), 9–15.

Berndt, T., et al., 2005. Rapid formation of sulfuric acid particles at near-atmospheric conditions. Science 307 (5710), 698–700.

Bianchi, F., et al., 2016. New particle formation in the free troposphere: a question of chemistry and timing. Science 352 (6289), 1109–1112.

Bianco, A., et al., 2016. Improving the characterization of dissolved organic carbon in cloud water: amino acids and their impact on the oxidant capacity. Sci. Rep. 6 (1), 37420.

Birmili, W., et al., 2000. Evolution of newly formed aerosol particles in the continental boundary layer: a case study including OH and H2SO4 measurements. Geophys. Res. Lett. 27 (15), 2205–2208.

Bone, R.G.A., Bader, R.F.W., 1996. Identifying and analyzing intermolecular bonding interactions in van der Waals molecules. J. Phys. Chem. 100 (26), 10892–10911.

Bork, N., et al., 2012. Structures and reaction rates of the gaseous oxidation of SO$_2$ by an O$_3$(H$_2$O)$_{0-5}$ cluster – a density functional theory investigation. Atmos. Chem. Phys. 12 (8), 3639–3652.

Bork, N., Du, L., Kjaergaard, H.G., 2014. Identification and characterization of the HCl–DMS gas phase molecular complex via infrared spectroscopy and electronic structure calculations. J. Phys. Chem. A 118 (8), 1384–1389.

Cai, R., Jiang, J., 2017. A new balance formula to estimate new particle formation rate: reevaluating the effect of coagulation scavenging. Atmos. Chem. Phys. 17 (20), 12659–12675.

Carroll, M.T., Chang, C., Bader, R.F.W., 1988. Prediction of the structures of hydrogen-bonded complexes using the laplacian of the charge density. Mol. Phys. 63 (3), 387–405.

Chen, J., et al., 2017. Interaction of oxalic acid with dimethylamine and its atmospheric implications. RSC Adv. 7 (11), 6374–6388.

Chu, B., et al., 2019. Atmospheric new particle formation in China. Atmos. Chem. Phys. 19 (1), 115–138.

Cornell, S.E., et al., 2003. Organic nitrogen deposition on land and coastal environments: a review of methods and data. Atmos. Environ. 37 (16), 2173–2191.

Dunne, E.M., et al., 2016. Global atmospheric particle formation from CERN CLOUD measurements. Science 354 (6316), 1119–1124.

Elm, J., Bilde, M., Mikkelsen, K.V., 2012. Assessment of density functional theory in predicting structures and free energies of reaction of atmospheric prenucleation clusters. J. Chem. Theor. Comput. 8 (6), 2071–2077.

Elm, J., et al., 2013. Interaction of glycine with common atmospheric nucleation precursors. J. Phys. Chem. A 117 (48), 12990–12997.

Elm, J., Bilde, M., Mikkelsen, K.V., 2013. Assessment of binding energies of atmospherically relevant clusters. Phys. Chem. Chem. Phys. 15 (39), 16442–16445.

Feltracco, M., et al., 2019. Free and combined L- and D-amino acids in Arctic aerosol. Chemosphere 220, 412–421.

Fenn, M.E., et al., 1998. Nitrogen excess in North American ecosystems: predisposing factors, ecosystem responses, and management strategies. Ecol. Appl. 8 (3), 706–733.

Gálvez, O., Gómez, P.C., Pacios, L.F., 2001. Variation with the intermolecular distance of properties dependent on the electron density in hydrogen bond dimers. J. Chem. Phys. 115 (24), 11166–11184.

Ge, X., Wexler, A.S., Clegg, S.L., 2011. Atmospheric amines – Part II. Thermodynamic properties and gas/particle partitioning. Atmos. Environ. 45 (3), 561–577.

Ge, P., et al., 2018. Molecular understanding of the interaction of amino acids with sulfuric acid in the presence of water and the atmospheric implication. Chemosphere 210, 215–223.

Herb, J., et al., 2013. Large hydrogen-bonded pre-nucleation (HSO$_4^-$)(H$_2$SO$_4$)$_m$(H$_2$O)$_k$ and (HSO$_4^-$)(NH$_3$)(H$_2$SO$_4$)$_m$(H$_2$O)$_k$ clusters in the earth's atmosphere. J. Phys. Chem. A 117 (1), 133–152.

Hostaš, J., Řezáč, J., Hobza, P., 2013. On the performance of the semiempirical quantum mechanical PM6 and PM7 methods for noncovalent interactions. Chem. Phys. Lett. 568–569, 161–166.

Huang, W., et al., 2010. Isomer identification and resolution in small gold clusters. J. Chem. Phys. 132 (5), 054305.

Huang, X., et al., 2018. Development and validation of a HPLC/FLD method combined with online derivatization for the simple and simultaneous determination of trace amino acids and alkyl amines in continental and marine aerosols. PloS One 13 (11), e0206488.

Humphrey, W., Dalke, A., Schulten, K., 1996. VMD: visual molecular dynamics. J. Mol. Graph. 14 (1), 33–38.

Ianni, J.C., Bandy, A.R., 1999. A density functional theory study of the hydrates of NH$_3$·H$_2$SO$_4$ and its implications for the formation of new atmospheric particles. J. Phys. Chem. A 103 (15), 2801–2811.

Jen, C.N., McMurry, P.H., Hanson, D.R., 2014. Stabilization of sulfuric acid dimers by ammonia, methylamine, dimethylamine, and trimethylamine. J. Geophys. Res.: Atmospheres 119 (12), 7502–7514.

Johnson, E.R., et al., 2010. Revealing noncovalent interactions. J. Am. Chem. Soc. 132 (18), 6498–6506.

Jokinen, T., et al., 2012. Atmospheric sulphuric acid and neutral cluster measurements using CI-APi-TOF. Atmos. Chem. Phys. 12 (9), 4117–4125.

Junninen, H., et al., 2010. A high-resolution mass spectrometer to measure atmospheric ion composition. Atmospheric Measurement Techniques 3 (4), 1039–1053.

Kalberer, M., et al., 2004. Identification of polymers as major components of atmospheric organic aerosols. Science 303 (5664), 1659–1662.

Kalivitis, N., et al., 2019. Formation and growth of atmospheric nanoparticles in the eastern Mediterranean: results from long-term measurements and process simulations. Atmos. Chem. Phys. 19 (4), 2671–2686.

Kim, J., et al., 1994. Entropy-driven structures of the water octamer. Chem. Phys. Lett. 219 (3), 243–246.

Kim, H., et al., 2019. Chemical processing of water-soluble species and formation of secondary organic aerosol in fogs. Atmos. Environ. 200, 158–166.

Knopf, D.A., Alpert, P.A., Wang, B., 2018. The role of organic aerosol in atmospheric ice nucleation: a review. ACS Earth and Space Chemistry 2 (3), 168–202.

Kontkanen, J., et al., 2018. Exploring the potential of nano-Köhler theory to describe the growth of atmospheric molecular clusters by organic vapors using cluster kinetics simulations. Atmos. Chem. Phys. 18 (18), 13733–13754.

Kourtchev, I., et al., 2009. Characterization of atmospheric aerosols at a forested site in central europe. Environ. Sci. Technol. 43 (13), 4665–4671.

Kuang, C., et al., 2008. Dependence of nucleation rates on sulfuric acid vapor concentration in diverse atmospheric locations. J. Geophys. Res.: Atmospheres 113 (D10), D10209.

Kulmala, M., 2003. How particles nucleate and grow. Science 302 (5647), 1000–1001.

Kulmala, M., et al., 2004. Formation and growth rates of ultrafine atmospheric particles: a review of observations. J. Aerosol Sci. 35 (2), 143–176.

Kurtén, T., et al., 2006. Ab initio and density functional theory reinvestigation of gas-phase sulfuric acid monohydrate and ammonium hydrogen sulfate. J. Phys. Chem. A 110 (22), 7178–7188.

Kurtén, T., et al., 2007. Estimating the NH 3: H 2 SO 4 ratio of nucleating clusters in atmospheric conditions using quantum chemical methods. Atmos. Chem. Phys. 7 (10), 2765–2773.

Kurtén, T., et al., 2008. Amines are likely to enhance neutral and ion-induced sulfuric acid-water nucleation in the atmosphere more effectively than ammonia. Atmos. Chem. Phys. 8 (14), 4095–4103.

Laskin, A., et al., 2003. Reactions at interfaces as a source of sulfate formation in sea-salt particles. Science 301 (5631), 340–344.

Lee, S.-H., et al., 2019. New particle formation in the atmosphere: from molecular clusters to global climate. J. Geophys. Res.: Atmospheres 124 (13), 7098–7146.

Leverentz, H.R., et al., 2013. Energetics of atmospherically implicated clusters made of sulfuric acid, ammonia, and dimethyl amine. J. Phys. Chem. A 117 (18), 3819–3825.

Li, J., et al., 2019. Hydration of acetic acid-dimethylamine complex and its atmospheric implications. Atmos. Environ. 219, 117005.

Lin, Y., et al., 2019. Interaction between succinic acid and sulfuric acid–base clusters. Atmos. Chem. Phys. 19 (12), 8003–8019.

Liu, Y.-R., et al., 2014. Structural exploration of water, nitrate/water, and oxalate/water clusters with Basin-Hopping method using a compressed sampling technique. J. Phys. Chem. A 118 (2), 508–516.

Loukonen, V., et al., 2010. Enhancing effect of dimethylamine in sulfuric acid nucleation in the presence of water – a computational study. Atmos. Chem. Phys. 10 (10), 4961–4974.

Lovejoy, E.R., Curtius, J., Froyd, K.D., 2004. Atmospheric ion-induced nucleation of sulfuric acid and water. J. Geophys. Res.: Atmospheres 109 (D8), D08204.

Lu, T., Chen, F., 2012. Multiwfn: a multifunctional wavefunction analyzer. J. Comput. Chem. 33 (5), 580–592.

Maia, J.D.C., et al., 2012. GPU linear algebra libraries and GPGPU programming for accelerating MOPAC semiempirical quantum chemistry calculations. J. Chem. Theor. Comput. 8 (9), 3072–3081.

Mandalakis, M., et al., 2011. Free and combined amino acids in marine background atmospheric aerosols over the Eastern Mediterranean. Atmos. Environ. 45 (4), 1003–1009.

Matos, J.T.V., Duarte, R.M.B.O., Duarte, A.C., 2016. Challenges in the identification and characterization of free amino acids and proteinaceous compounds in atmospheric aerosols: a critical review. Trac. Trends Anal. Chem. 75, 97–107.

McGrath, M.J., et al., 2012. Atmospheric Cluster Dynamics Code: a flexible method for solution of the birth-death equations. Atmos. Chem. Phys. 12 (5), 2345–2355.

Milne, P.J., Zika, R.G., 1993. Amino acid nitrogen in atmospheric aerosols: occurrence, sources and photochemical modification. J. Atmos. Chem. 16 (4), 361–398.

Nadykto, A.B., Yu, F., 2007. Strong hydrogen bonding between atmospheric nucleation precursors and common organics. Chem. Phys. Lett. 435 (1), 14–18.

Nadykto, A., Yu, F., Herb, J., 2008. Effect of ammonia on the gas-phase hydration of the common atmospheric ion HSO$_4$. Int. J. Mol. Sci. 9 (11), 2184–2193.

Nieminen, T., et al., 2009. Connection of sulfuric acid to atmospheric nucleation in boreal forest. Environ. Sci. Technol. 43 (13), 4715–4721.

Ortega, I.K., et al., 2008. The role of ammonia in sulfuric acid ion induced nucleation. Atmos. Chem. Phys. 8 (11), 2859–2867.

Ortega, I.K., et al., 2012. From quantum chemical formation free energies to evaporation rates. Atmos. Chem. Phys. 12 (1), 225–235.

Ren, L., et al., 2018. Molecular composition and seasonal variation of amino acids in urban aerosols from Beijing, China. Atmos. Res. 203, 28–35.

Roosta, H., et al., 2018. The dual effect of amino acids on the nucleation and growth rate of gas hydrate in ethane+ water, methane+ propane+ water and methane+ THF+ water systems. Fuel 212, 151–161.

Rozas, I., Alkorta, I., Elguero, J., 2000. Behavior of ylides containing N, O, and C atoms as hydrogen bond acceptors. J. Am. Chem. Soc. 122 (45), 11154–11161.

Saikia, J., et al., 2016. Nanominerals, fullerene aggregates, and hazardous elements in coal and coal combustion-generated aerosols: an environmental and toxicological assessment. Chemosphere 164, 84–91.

Saxon, A., Diaz-Sanchez, D., 2005. Air pollution and allergy: you are what you breathe. Nat. Immunol. 6 (3), 223–226.

Scheller, E., 2001. Amino acids in dew – origin and seasonal variation. Atmos. Environ. 35 (12), 2179–2192.

Schobesberger, S., et al., 2013. Molecular understanding of atmospheric particle formation from sulfuric acid and large oxidized organic molecules. Proc. Natl. Acad. Sci. Unit. States Am. 110 (43), 17223–17228.

Seinfeld, J.H., Pandis, S.N., 2006. Atmospheric Chemistry and Physics: from Air Pollution to Climate Change.

Sipilä, M., et al., 2010a. The role of sulfuric acid in atmospheric nucleation. Science 327 (5970), 1243–1246.

Sipilä, M., et al., 2010b. The role of sulfuric acid in atmospheric nucleation. Science 327 (5970), 1243–1246.

Smith, J.N., et al., 2008. Chemical composition of atmospheric nanoparticles formed from nucleation in Tecamac, Mexico: evidence for an important role for organic species in nanoparticle growth. Geophys. Res. Lett. 35 (4), L04808.

Stinson, J.L., Kathmann, S.M., Ford, I.J., 2016. A classical reactive potential for molecular clusters of sulphuric acid and water. Mol. Phys. 114 (2), 172–185.

Temelso, B., Phan, T.N., Shields, G.C., 2012. Computational study of the hydration of sulfuric acid dimers: implications for acid dissociation and aerosol formation. J. Phys. Chem. A 116 (39), 9745–9758.

Vaattovaara, P., et al., 2006. The composition of nucleation and Aitken modes particles during coastal nucleation events: evidence for marine secondary organic contribution. Atmos. Chem. Phys. 6 (12), 4601–4616.

Vehkamäki, H., et al., 2002. An improved parameterization for sulfuric acid–water nucleation rates for tropospheric and stratospheric conditions. J. Geophys. Res.: Atmospheres 107 (D22). AAC 3-1-AAC 3-10.

Wales, D.J., Doye, J.P.K., 1997. Global optimization by Basin-Hopping and the lowest energy structures of Lennard-Jones clusters containing up to 110 atoms. J. Phys. Chem. A 101 (28), 5111–5116.

Wang, C.-Y., et al., 2016. Bidirectional interaction of alanine with sulfuric acid in the presence of water and the atmospheric implication. J. Phys. Chem. A 120 (15), 2357–2371.

Weber, R.J., et al., 1996. Measured atmospheric new particle formation rates: implications for nucleation mechanisms. Chem. Eng. Commun. 151 (1), 53–64.

Weber, R.J., et al., 1999. New particle formation in the remote troposphere: a comparison of observations at various sites. Geophys. Res. Lett. 26 (3), 307–310.

Wen, H., et al., 2018. A study on the microscopic mechanism of methanesulfonic acid-promoted binary nucleation of sulfuric acid and water. Atmos. Environ. 191, 214–226.

Wu, F.C., Tanoue, E., 2002. Tryptophan in the sediments of lakes from southwestern China plateau. Chem. Geol. 184 (1), 139–149.

Xu, Y., et al., 2010. Formation and properties of hydrogen-bonded complexes of common organic oxalic acid with atmospheric nucleation precursors. J. Mol. Struct.: THEOCHEM 951 (1), 28–33.

Xu, J., Finlayson-Pitts, B.J., Gerber, R.B., 2017. Proton transfer in mixed clusters of methanesulfonic acid, methylamine, and oxalic acid: implications for atmospheric particle formation. J. Phys. Chem. A 121 (12), 2377–2385.

Xu, C.-X., et al., 2020. Formation of atmospheric molecular clusters of methanesulfonic acid–Diethylamine complex and its atmospheric significance. Atmos. Environ. 226, 117404.

Zhang, Q., Anastasio, C., 2001. Chemistry of fog waters in California's Central Valley—Part 3: concentrations and speciation of organic and inorganic nitrogen. Atmos. Environ. 35 (32), 5629–5643.

Zhang, Q., Anastasio, C., 2003. Free and combined amino compounds in atmospheric fine particles (PM2.5) and fog waters from Northern California. Atmos. Environ. 37 (16), 2247–2258.

Zhang, Q., Anastasio, C., Jimenez-Cruz, M., 2002. Water-soluble organic nitrogen in atmospheric fine particles (PM2.5) from northern California. J. Geophys. Res.: Atmospheres 107 (D11). AAC 3-1-AAC 3-9.

Zhang, R., et al., 2004. Atmospheric new particle formation enhanced by organic acids. Science 304 (5676), 1487–1490.

Zhang, R., et al., 2007. Intensification of Pacific storm track linked to Asian pollution. Proc. Natl. Acad. Sci. Unit. States Am. 104 (13), 5295–5299.

Zhang, R., et al., 2012. Nucleation and growth of nanoparticles in the atmosphere. Chem. Rev. 112 (3), 1957–2011.

Zhang, H., et al., 2018. The potential role of malonic acid in the atmospheric sulfuric acid - ammonia clusters formation. Chemosphere 203, 26–33.

Zhao, Y., Truhlar, D.G., 2008. The M06 suite of density functionals for main group thermochemistry, thermochemical kinetics, noncovalent interactions, excited states, and transition elements: two new functionals and systematic testing of four M06-class functionals and 12 other functionals. Theoretical Chemistry Accounts 120 (1–3), 215–241.

Zhao, J., et al., 2010. Chemical ionization mass spectrometric measurements of atmospheric neutral clusters using the cluster-CIMS. J. Geophys. Res.: Atmospheres 115 (D8), D08205.

Zhao, F., et al., 2019. Enhancement of atmospheric nucleation by highly oxygenated organic molecules: a density functional theory study. J. Phys. Chem. A 123 (25), 5367–5377.